

International Journal of Modern Physics B
 © World Scientific Publishing Company

The sawtooth chain: From Heisenberg spins to Hubbard electrons

J. RICHTER

*Institut für Theoretische Physik, Otto-von-Guericke Universität Magdeburg,
 P.O.Box 4120, 39016 Magdeburg, Germany
 www.uni-magdeburg.de/itp*

O. DERZHKO

*Institute for Condensed Matter Physics of the National Academy of Sciences of Ukraine,
 1 Svientsitskii Street, L'viv-11, 79011, Ukraine*

A. HONECKER

*Institut für Theoretische Physik, Georg-August-Universität Göttingen,
 37077 Göttingen, Germany*

Received February 10, 2019

We report on recent studies of the spin-half Heisenberg and the Hubbard model on the sawtooth chain. For both models we construct a class of exact eigenstates which are localized due to the frustrating geometry of the lattice for a certain relation of the exchange (hopping) integrals. Although these eigenstates differ in details for the two models because of the different statistics, they share some characteristic features. The localized eigenstates are highly degenerate and become ground states in high magnetic fields (Heisenberg model) or at certain electron fillings (Hubbard model), respectively. They may dominate the low-temperature thermodynamics and lead to an extra low-temperature maximum in the specific heat. The ground-state degeneracy can be calculated exactly by a mapping of the manifold of localized ground states onto a classical hard-dimer problem, and explicit expressions for thermodynamic quantities can be derived which are valid at low temperatures near the saturation field for the Heisenberg model or around a certain value of the chemical potential for the Hubbard model, respectively.

Keywords: frustration, Heisenberg model, Hubbard model, localized eigenstates

1. Introduction

Frustrated lattices play an important role in the search for exotic quantum states of condensed matter. The term ‘frustration’ was introduced in physics in the 1970s by Toulouse [1] in the context of spin glasses [2] and describes a situation where exchange interactions are in competition with each other. The studies on spin glasses have demonstrated that frustration may have an enormous influence on ground-state and thermodynamic properties of spin systems [2].

In the 1970s Anderson and Fazekas [3] first considered the quantum spin-1/2 Heisenberg antiferromagnet on the geometrically frustrated triangular lattice and

proposed a liquid-like ground state without magnetic long-range order. Although later on it was found that the spin-1/2 Heisenberg antiferromagnet on the triangular lattice possesses semi-classical three-sublattice Néel order (see, e.g., Refs. [4, 5] for recent reviews), Anderson’s suggestion was the starting point to search for exotic quantum ground states in frustrated spin systems.

The recent progress in synthesizing frustrated magnetic materials with strong quantum fluctuations [6] and the rich behavior of such magnetic systems have stimulated an enormous interest in frustrated quantum magnets, see, e.g., Refs. [7–11]. There are many compounds which correspond to quantum antiferromagnetic Heisenberg models with frustrated spin interactions. We mention as examples the frustrated spin-1/2 $J_1 - J_2$ chains ($\text{Rb}_2\text{Cu}_2\text{Mo}_3\text{O}_{12}$, LiCuVO_4 , $\text{Li}_2\text{ZrCuO}_4$) [12] and the kagomé lattice ($\text{ZnCu}_3(\text{OH})_6\text{Cl}_2$) [13]. There are also compounds which correspond to electronic (Hubbard, $t - J$, periodic Anderson) models on geometrically frustrated lattices. We mention as examples cobaltates [14], CeRh_3B_2 [15], as well as artificial crystals from quantum dots [16].

In this paper we will focus on a special property of the Heisenberg and the Hubbard model on a particular geometrically frustrated lattice (the sawtooth chain, see Fig. 1), namely the existence of localized eigenstates (on a perfect lattice) and their relevance for the low-temperature physics of those correlated systems. Note, however, that arguments and calculations presented in this paper can in principle be applied to wide class of frustrated lattices, see the discussion below and Refs. [17–28].

In general, for perfect lattices an elementary excitation as a non-interacting quasiparticle is spread over the entire lattice. For example, for a simple hypercubic lattice a magnon or electron wave function is extended over all lattice sites due to a hopping term in the Hamiltonian. However, for some lattice geometries a wave function of an elementary excitation in a quantum system may have amplitudes which are non-zero only in a restricted area owing to destructive quantum interference. We call such excitations localized excitations (for example, localized magnons [17–19] or localized electron states [25–30]). Due to the local character of these excitations exact many-particle eigenstates of the Hamiltonian can be built by n independent localized excitations (i.e. they have a sufficiently large separation between each other) even in the presence of interactions. The number n of localized excitations cannot exceed a certain maximal value n_{\max} which depends on the specific lattice under consideration, where n_{\max} is proportional to the system size N [18, 28]. If the localized excitation is the lowest-energy eigenstate of the Hamiltonian in the one-particle subspace one may expect that a state with n independent (isolated) localized excitations is the lowest-energy eigenstate of the Hamiltonian in the corresponding n -particle subspace [17, 18, 28, 31] provided there is no attractive interaction. The localized eigenstates may become ground states in high magnetic fields (Heisenberg model) or at certain electron fillings (Hubbard model), respectively. Therefore they may substantially contribute to or even completely dominate the low-temperature thermodynamic properties of the system.

In the present paper we discuss the effect of localized elementary excitations on

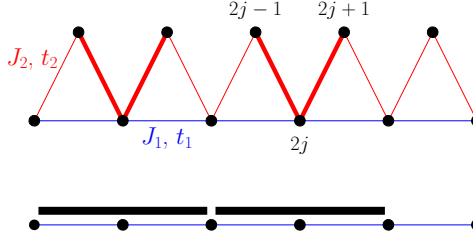


Fig. 1. (Color online) Upper part: the sawtooth chain. Filled circles indicate the lattice sites, lines indicate the exchange/hopping bonds. Two trapping cells occupied by localized magnons/electrons are indicated by bold lines. Note that for the sawtooth chain one has two kinds of bonds of different strength. The lower part of the figure indicates the corresponding hard-dimer model (two hard dimers on a linear chain).

the low-temperature thermodynamics focusing on the quantum Heisenberg antiferromagnet and the Hubbard model on the sawtooth chain. We follow the lines which have been developed in a series of papers on localized eigenstates for the Heisenberg model [5, 17–24, 31–42] and for electronic models [25–30].

To be specific we consider the Heisenberg antiferromagnet of N spins with quantum number $s = 1/2$ in a magnetic field h

$$H = \sum_{\langle i,j \rangle} J_{ij} \vec{s}_i \cdot \vec{s}_j - h S^z \quad (1)$$

and the Hubbard model of N lattice sites

$$H = \sum_{\substack{\langle i,j \rangle \\ \sigma=\uparrow,\downarrow}} t_{ij} \left(c_{i,\sigma}^\dagger c_{j,\sigma} + c_{j,\sigma}^\dagger c_{i,\sigma} \right) + U \sum_i n_{i,\uparrow} n_{i,\downarrow} + \mu \sum_{i,\sigma=\uparrow,\downarrow} n_{i,\sigma}. \quad (2)$$

In (1) and (2) the first sum runs over all neighboring sites on the lattice under consideration, $J_{ij} > 0$ is the antiferromagnetic isotropic Heisenberg exchange interaction between the sites i and j , and $S^z = \sum_i s_i^z$ is the z -component of the total spin. In (2) $t_{ij} > 0$ is the hopping matrix element between the nearest-neighbor sites i and j , $U > 0$ is the on-site Coulomb repulsion, μ is the chemical potential, and $n_{i,\sigma} = c_{i,\sigma}^\dagger c_{i,\sigma}$. For electronic models the chemical potential μ plays the role of the magnetic field h . While for the Heisenberg antiferromagnet h controls the magnetization $M = S^z$, μ controls the average number of electrons in the system for the Hubbard model.

In what follows we first consider the frustrated quantum Heisenberg antiferromagnet on the sawtooth chain (Fig. 1) and discuss some generic properties of the model which are caused by the localized magnon states. In particular, we consider the magnetization process, calculate the ground-state degeneracy of the localized eigenstates leading to a finite residual entropy and discuss the low-temperature thermodynamics for magnetic fields in the vicinity of the saturation field (Sec. 2). Then we illustrate the application of the concepts elaborated for the spin system to the

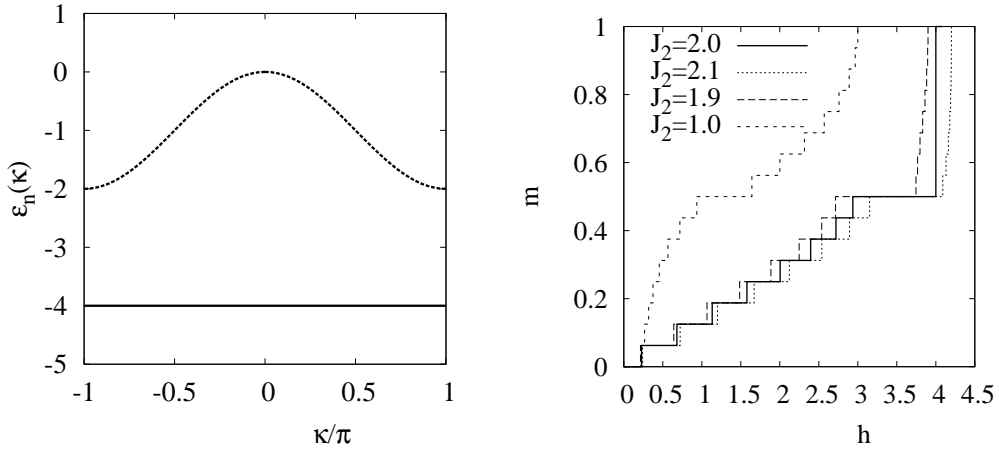


Fig. 2. Left: One-magnon dispersion for the spin-1/2 Heisenberg antiferromagnet on the sawtooth chain with $J_2 = 2$, $J_1 = 1$ and $h = 0$ (cf. Eq. (3)). Right: Ground-state magnetization curves $m(h) = M(h)/M_{\max}$ for the spin-1/2 Heisenberg antiferromagnet on the sawtooth chain for various values of J_2 and $J_1 = 1$.

Hubbard model on the sawtooth chain in Sec. 3. Sec. 4 presents a short summary of our discussion.

2. Localized Magnon States in the Heisenberg Antiferromagnet on the Sawtooth Chain

2.1. Flat bands and localized eigenstates

In this section we illustrate how the localized magnon states emerge for the frustrated quantum Heisenberg antiferromagnet (1). The fact that S^z commutes with the Hamiltonian (1) permits us to consider the eigenstates separately in each subspace with different values of $S^z = N/2, N/2-1, \dots$. In the subspace with $S^z = N/2$ the only eigenstate is the fully polarized ferromagnetic state, $|\text{FM}\rangle = |\uparrow\uparrow\uparrow\uparrow\dots\rangle$, which plays the role of the vacuum state for the magnon excitations.

In the one-magnon subspace ($S^z = N/2 - 1$) it is simple to calculate the eigenstates given by $|1_\kappa\rangle = \sum_{l=0}^1 c_l \sum_{j=1}^{N/2} e^{i\kappa j} s_{2j+l}^- |\text{FM}\rangle$; $H|1_\kappa\rangle = \varepsilon_\pm(\kappa)|1_\kappa\rangle$. The two one-magnon branches are given by

$$\varepsilon_\pm(\kappa) = h - \frac{J_1 + 2J_2}{2} + \frac{1}{2} \left[J_1 \cos \kappa \pm \sqrt{J_1^2 (-1 + \cos \kappa)^2 + 2J_2^2 (1 + \cos \kappa)} \right]. \quad (3)$$

For $J_2 = 2J_1$, the lower magnon band becomes completely flat, i.e. $\varepsilon_-(\kappa) = \varepsilon_- = h - 4J_1$, see the left panel of Fig. 2. Let us now focus on the case $J_2 = 2J_1$. A dispersionless band allows one to construct localized excitations given here by $|1lm\rangle = l_{2j}^\dagger |\text{FM}\rangle$, where $l_{2j}^\dagger = (1/\sqrt{6}) (s_{2j-1}^- - 2s_{2j}^- + s_{2j+1}^-)$ creates a spin excitation (magnon) localized in a valley (trapping cell) indicated by bold lines in the

upper part of Fig. 1. Note that a typical geometrical feature of a lattice leading to the possibility to localize eigenstates is a triangular configuration of antiferromagnetic bonds, where the triangle is built by one bond of the trapping cell (here a valley) and two bonds attached to the trapping cell [18, 19], see Fig. 1.

Let us consider the n -magnon subspace with $S^z = N/2 - n$. In this subspace the construction of the eigenstates of the Heisenberg model is, generally, a difficult many-body problem. However, for a lattice which supports localized magnon states, a state $|nlm\rangle$ consisting of n independent (i.e. isolated) localized magnons is an exact eigenstate of the Hamiltonian (1). Using the l^\dagger -operators introduced above these states can be written as $|nlm\rangle = l_{i_1}^\dagger l_{i_2}^\dagger \dots l_{i_n}^\dagger |FM\rangle$, where the i_l are sufficiently separated lattice sites. For the sawtooth chain all n localized magnons are independent (isolated) if they do not occupy neighboring valleys (hard core rule). This constraint immediately leads to a maximum number of localized magnons $n_{\max} = N/4$. The energy of the n -particle state $|nlm\rangle$ is

$$E_{nlm} = E_{FM} - \frac{N}{2}h + n(h - 4J_1), \quad (4)$$

i.e. at $h = h_1 = 4J_1$ all localized magnon states are degenerate. It is important to note that the localized magnon states are the lowest eigenstates in all sectors of $S^z = N/2 - 1, N/2 - 2, \dots, N/2 - n_{\max}$ [17, 31]. Hence these states become ground states in an appropriate magnetic field. Furthermore it can be shown that all localized magnon states are linearly independent for the sawtooth chain [38] and that the localized magnon states present the complete manifold of ground states in all relevant sectors of S^z [21, 22, 24].

In the following sections we will discuss how the localized eigenstates influence the physical properties of frustrated lattices.

2.2. Plateaus and jumps in the magnetization curve

First we consider the relevance of the localized magnon states for the magnetization process. For the calculation of the magnetization $M = S^z$ at $T = 0$ it is sufficient to find the lowest energy levels $E(M)$ in the subspaces with different $M = N/2, N/2 - 1, \dots$ for $h = 0$. The energy in the presence of an external magnetic field h is given by $E(M, h) = E(M) - hM$, where the magnetization M should acquire a value which minimizes $E(M, h)$. Hence M can be determined from the equation $dE(M)/dM = h$ which finally gives the magnetization curve $m(h)$ where $m = M/M_{\max}$, $M_{\max} = N/2$. For a classical non-frustrated Heisenberg antiferromagnet one typically finds a parabolic relation $E(M) \propto M^2$ resulting in a straight-line behavior $M \propto h$. Often quantum fluctuations lead only to small deviations from a linear $M - h$ relation, see, e.g., Refs. [4, 5, 43]. However, in the presence of frustration and quantum fluctuations more exotic magnetization curves, e.g., curves with plateaus, can be observed [4, 5, 43]. Another spectacular feature observed in magnetization curves of frustrated quantum spin systems consists in discontinuous jumps related to a linear relation $E \propto M$ [5, 17–19, 24, 44]. As discussed in the previous section we find such

a linear $E - M$ relation for the sawtooth Heisenberg antiferromagnet with $J_2 = 2J_1$ for values of the magnetization for which the lowest eigenstates are localized states, see Eq. (4). This leads to a magnetization jump from $m = 1/2$ directly to saturation $m = 1$ at the saturation field $h_1 = 4J_1$, see the right panel of Fig. 2. In addition there is wide plateau preceding the jump. This plateau state represents a regular pattern of alternately occupied and empty valleys and is two-fold degenerate. Magnetization curves with a jump to saturation for other lattices can be found, e.g., in Refs. [17–19, 33, 37, 40, 43–45]. We emphasize that the jump is macroscopic, and that there is no finite-size effect. Furthermore we mention that a jump to saturation can be found also for the sawtooth Heisenberg antiferromagnet with higher spin quantum number $s > 1/2$. However, the height of the jump decreases with $1/s$, i.e. the jump is a true quantum effect and disappears in the classical limit $s \rightarrow \infty$.

Finally, let us discuss deviations from the ideal parameter constellation $J_2 = 2J_1$ for which the localized magnon states are true eigenstates. The right panel of Fig. 2 shows that small deviations (e.g., $J_2 = 1.9J_1$, $J_2 = 2.1J_1$) do not change the magnetization curve drastically, whereas the model with uniform bonds $J_2 = J_1$ exhibits a qualitatively different $m(h)$ behavior.

2.3. *Ground-state residual entropy and low-temperature thermodynamics*

It has been shown above that the energy of the n -magnon state in a magnetic field is $E_{\text{FM}} - Nh/2 + n(h - 4J_1)$, cf. Eq. (4). Obviously, for $n < n_{\text{max}}$ this energy level is highly degenerate, since there are many ways to place n independent localized magnons on a lattice. The degeneracy further increases at the saturation field $h_1 = 4J_1$, since the energies of the states with different numbers of localized magnons $n = 0, 1, \dots, n_{\text{max}}$ become equal, namely $E_{\text{FM}} - Nh_1/2$. We denote this degeneracy at $h = h_1$ by \mathcal{W} . Since all localized magnon states are linearly independent [38], they span a highly degenerate ground-state manifold at $h = h_1$. The degree of degeneracy can be calculated by taking into account the hard-core rule (simultaneous occupation of neighboring valleys by localized magnons is forbidden). The remaining counting problem can be solved by mapping the localized magnon problem on the sawtooth chain with N sites onto a hard-dimer problem (simultaneous occupation of neighboring sites by dimers is forbidden) on a simple linear chain with $\mathcal{N} = N/2$ sites, see the lower part of Fig. 1 and also Refs. [20–22, 24]. Taking the number of hard-dimer distributions from the literature [46] we can use this mapping to find the ground-state degeneracy at the saturation field \mathcal{W} . For $\mathcal{N} \rightarrow \infty$ one finds $\mathcal{W} = ((1 + \sqrt{5})/2)^{\mathcal{N}} \approx \exp(0.4812\mathcal{N})$ leading to a finite residual entropy of $S/k_B N = (1/2) \ln((1 + \sqrt{5})/2) \approx 0.2406$ for the sawtooth chain with $J_2 = 2J_1$ at $h = h_1$ [20–22].

In addition, we can use the correspondence between the localized magnon states and the spatial configurations of hard dimers to calculate the contribution of the localized magnon states to the thermodynamic quantities following the lines given,

e.g., in Refs. [46,47]. This contribution may dominate the low-temperature thermodynamics and therefore we may find predictions for the low-temperature behavior of the magnetic quantities in the vicinity of the saturation field h_1 . The contribution of the localized states to the partition function of the spin model can be written as

$$\begin{aligned} Z_{\text{lm}}(T, h, N) &= \exp \left(-\frac{E_{\text{FM}} - h \frac{N}{2}}{k_B T} \right) \sum_{n=0}^{n_{\text{max}}} g_N(n) \exp \left(\frac{h_1 - h}{k_B T} n \right) \\ &= \exp \left(-\frac{E_{\text{FM}} - h \frac{N}{2}}{k_B T} \right) \Xi(T, \mu, \mathcal{N}) ; \quad \mathcal{N} = \frac{N}{2}. \end{aligned} \quad (5)$$

Here $g_N(n)$ is the degeneracy of the ground state of the spin model with N sites in the sector with n localized magnons, i.e. with $M = S^z = N/2 - n$. In the hard-dimer description $g_N(n)$ corresponds to the canonical partition function $Z(n, \mathcal{N})$ of the classical hard-dimer model. $h_1 - h = \mu$ is the chemical potential of the hard dimers and $\Xi(T, \mu, \mathcal{N})$ (or $\Xi(z, \mathcal{N})$, $z = \exp(\mu/k_B T)$) is the grand-canonical partition function of the one-dimensional hard-dimer lattice gas given by

$$\Xi(T, \mu, \mathcal{N}) = \lambda_1^{\mathcal{N}} + \lambda_2^{\mathcal{N}}, \quad \lambda_{1,2} = \frac{1}{2} \pm \sqrt{\frac{1}{4} + \exp x}, \quad x = \frac{\mu}{k_B T}. \quad (6)$$

Formula (5) describes the low-temperature thermodynamics of the spin model near the saturation field accurately, i.e. $Z(T, h, N) \approx Z_{\text{lm}}(T, h, N)$, because of the huge degeneracy of the ground state at $h = h_1$ (note that there are no other ground states apart from the considered localized-magnon states in the corresponding sectors of S^z). We mention that similar considerations are possible for other frustrated lattices [21–24, 39, 41, 42]. The contribution of the localized magnon states to the Helmholtz free energy F of the spin model is given by $F_{\text{lm}}(T, h, N)/N = E_{\text{FM}}/N - h/2 - k_B T \ln \Xi(z, \mathcal{N})/N$. The entropy S , the specific heat C , the magnetization M and the susceptibility χ follow from $F_{\text{lm}}(T, h, N)$ according to usual relations $S_{\text{lm}}(T, h, N) = -\partial F_{\text{lm}}(T, h, N)/\partial T$, $C_{\text{lm}}(T, h, N) = T \partial S_{\text{lm}}(T, h, N)/\partial T$, $M_{\text{lm}}(T, h, N) = N/2 - \langle n \rangle = N/2 - k_B T \partial \ln \Xi(T, \mu, \mathcal{N})/\partial \mu$, $\chi_{\text{lm}}(T, h, N) = \partial M_{\text{lm}}(T, h, N)/\partial h$. In the limit $N \rightarrow \infty$ this leads to [20, 23, 24]

$$\begin{aligned} \frac{S_{\text{lm}}(T, h, N)}{k_B N} &= \frac{1}{2} \left[\ln \left(\frac{1}{2} + \sqrt{\frac{1}{4} + \exp x} \right) - x \left(\frac{1}{2} - \frac{1}{4\sqrt{\frac{1}{4} + \exp x}} \right) \right], \\ \frac{C_{\text{lm}}(T, h, N)}{k_B N} &= \frac{1}{16} \frac{x^2 \exp x}{\left(\frac{1}{4} + \exp x \right)^{\frac{3}{2}}}, \\ \frac{M_{\text{lm}}(T, h, N)}{\frac{N}{2}} &= 1 - \left(\frac{1}{2} - \frac{1}{4\sqrt{\frac{1}{4} + \exp x}} \right), \\ \frac{k_B T \chi_{\text{lm}}(T, h, N)}{N} &= \frac{1}{16} \frac{\exp x}{\left(\frac{1}{4} + \exp x \right)^{\frac{3}{2}}}; \quad x = \frac{\mu}{k_B T} = \frac{h_1 - h}{k_B T}. \end{aligned} \quad (7)$$

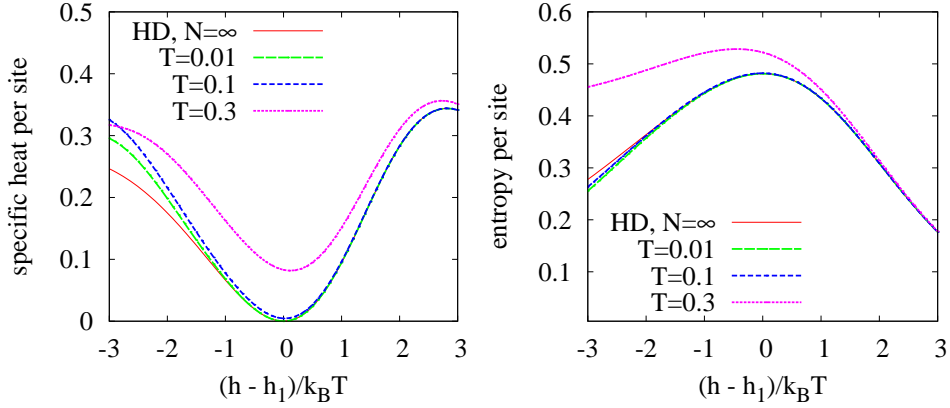


Fig. 3. (Color online) The specific heat (left) and the entropy (right) in dependence on $x = (h_1 - h)/k_B T$ for the spin-1/2 Heisenberg antiferromagnet on the sawtooth chain with $N = 20$, $J_1 = 1$, $J_2 = 2$ and $k_B T = 0.01, 0.1, 0.3$ in comparison with the one-dimensional hard-dimer (HD) gas, Eq. (7).

The thermodynamic quantities depend on T and h via the universal parameter $x = (h_1 - h)/k_B T$ only. Corresponding formulas for finite systems can be found using $\Xi(T, \mu, \mathcal{N})$ from Eq. (6) in combination with the relation between $F_{lm}(T, h, N)$ and $\Xi(T, \mu, \mathcal{N})$ given above.

Fig. 3 shows a comparison of the entropy and the specific heat of the spin model in dependence on the universal parameter $x = (h_1 - h)/k_B T$ with the hard-dimer formulas. In addition we show the specific heat as an important measurable quantity in dependence on the temperature for magnetic fields slightly above and below the saturation field in Fig. 4.

We emphasize here some prominent features: an extra low-temperature peak in the dependence C vs. T for fields slightly below or slightly above h_1 (Figs. 3 and 4) and an enhanced entropy at h_1 at low temperatures (Fig. 3). Note that C in Eq. (7) is zero at $x = 0$ and consequently there is no extra peak in $C(T)$ for $h = h_1$, see also Fig. 3 (left). Furthermore from Figs. 3 and 4 it becomes evident that the hard-dimer description works excellently for temperatures up to 10% of the exchange coupling and reproduces qualitatively the characteristic features of the spin model for higher temperatures up to about $0.3J_1$.

Similar as for the magnetization curve we consider now the influence of deviations from the ideal parameter constellation $J_2 = 2J_1$ (for which the localized magnon states are true exact eigenstates) on thermodynamic quantities. From Fig. 4 it is obvious that only large deviations suppress the extra low-temperature peak in $C(T)$. This behavior can be explained by inspection of the low-energy spectrum. For small deviations the energy is only slightly changed and the originally highly degenerate ground-state manifold becomes quasi-degenerate. As a result the δ -peak

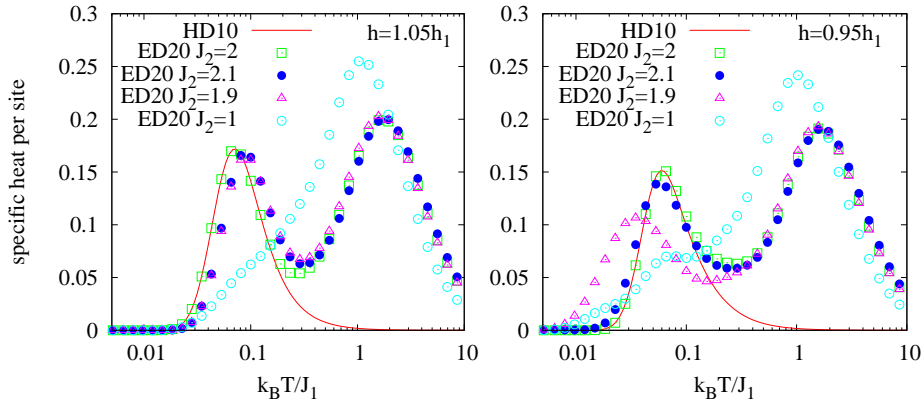


Fig. 4. (Color online) Temperature dependence of the specific heat for the spin-1/2 Heisenberg antiferromagnet on the sawtooth chain with $N = 20$, $J_1 = 1$ and various J_2 for magnetic fields slightly above ($h = 1.05h_1$, left) and below ($h = 0.95h_1$, right) the saturation field ($h_1 = 4, 4.2, 3.9$ and 3 for $J_2 = 2, 2.1, 1.9$ and 1 , respectively). For comparison we show the results for the one-dimensional hard-dimer (HD) gas with $\mathcal{N} = 10$ sites.

present in the low-energy density of states for $J_2 = 2J_1$ is broadened but there is still a well pronounced maximum in the density of states leading to the extra low- T peak in $C(T)$.

Let us very briefly discuss an aspect of the localized magnon scenario which might have some relevance for a possible application of highly frustrated magnets. Due to the huge degeneracy of the localized magnon states and the resulting residual entropy at $h = h_1$ there is a well pronounced low-temperature peak in the entropy S versus field h curve, see Fig. 3 (right). It has been pointed out first by Zhitomirsky [48] considering the classical kagomé Heisenberg antiferromagnet that such a degeneracy leads to an enhanced magnetocaloric effect. Later on this point has been discussed for quantum spin systems, e.g., in Refs. [20, 23, 24, 49].

3. Hubbard Electrons on the Sawtooth Chain

3.1. Flat one-electron band and localized electron eigenstates

We consider now the Hubbard model (2) on a sawtooth chain. The specific Hamiltonian reads

$$H = \sum_{j=0}^{\frac{N}{2}-1} \sum_{\sigma=\uparrow,\downarrow} \left[t_1 c_{2j,\sigma}^\dagger c_{2j+2,\sigma} + t_2 (c_{2j,\sigma}^\dagger c_{2j+1,\sigma} + c_{2j+1,\sigma}^\dagger c_{2j+2,\sigma}) + \text{h.c.} \right. \\ \left. + \mu (n_{2j,\sigma} + n_{2j+1,\sigma}) \right] + U \sum_{j=0}^{\frac{N}{2}-1} (n_{2j,\uparrow} n_{2j,\downarrow} + n_{2j+1,\uparrow} n_{2j+1,\downarrow}), \quad (8)$$

where $t_1 > 0$ and $t_2 > 0$ are the hopping integrals along the base line and the zig-zag path, respectively (see the upper part of Fig. 1), and $U > 0$ is the on-site Coulomb repulsion. The sawtooth-chain Hubbard model has attracted much attention since the 1990s [50]. Here we focus on a special aspect, namely the existence of localized ground states and their consequences for the low-temperature physics of the model. On the one-particle level the description of the electron system is the same as of the XY spin system [26–28]. The one-electron dispersion reads

$$\varepsilon_{\pm}(\kappa) = \mu + t_1 \cos \kappa \pm \sqrt{t_1^2 \cos^2 \kappa + 2t_2^2 (1 + \cos \kappa)} . \quad (9)$$

Thus, if $t_2 = \sqrt{2}t_1$ the lowest single electron energy becomes $\varepsilon_- = \mu - 2t_1$, i.e. it is completely flat. Similar as for the Heisenberg model we can construct N localized one-electron ground states, given by $l_{2j,\sigma}^{\dagger}|0\rangle$, $l_{2j,\sigma}^{\dagger} = (1/2)(c_{2j-1,\sigma}^{\dagger} - \sqrt{2}c_{2j,\sigma}^{\dagger} + c_{2j+1,\sigma}^{\dagger})$ (i.e. the electron is localized in any of the $N/2$ valleys labeled by the index $2j$ and having either spin up or spin down) with energy $\varepsilon_- = -2t_1 + \mu$. Note that the indices of the l^{\dagger} and c^{\dagger} operators correspond to the lattice sites as illustrated in Fig. 1.

The Hubbard repulsion becomes relevant in the two-electron subspace. Obviously, a two-particle ground state can be constructed by two independent localized electrons with arbitrary spin trapped on two valleys which do not touch each other. However, in contrast to the Heisenberg model there is no ‘hard-core rule’, i.e. there are further two-particle ground states with two electrons trapped on two neighboring valleys, e.g., with indices $2j$ and $2j+2$. The energy of the corresponding eigenstates $l_{2j,\uparrow}^{\dagger}l_{2j+2,\uparrow}^{\dagger}|0\rangle$ and $l_{2j,\downarrow}^{\dagger}l_{2j+2,\downarrow}^{\dagger}|0\rangle$ is also independent of U , since both electrons have the same spin and therefore the Pauli principle forbids the simultaneous occupation of the site $2j+1$ belonging to both valleys. In addition, a straightforward direct calculation shows that for two electrons having different spin the linear combination

$$l_{2j,\uparrow}^{\dagger}l_{2j+2,\downarrow}^{\dagger}|0\rangle + l_{2j,\downarrow}^{\dagger}l_{2j+2,\uparrow}^{\dagger}|0\rangle, \quad (10)$$

is also a ground state in the two-electron subspace with an energy independent of U . This can be seen also by using the SU(2) symmetry of the Hubbard Hamiltonian: the state (10) and the states $l_{2j,\uparrow}^{\dagger}l_{2j+2,\uparrow}^{\dagger}|0\rangle$ and $l_{2j,\downarrow}^{\dagger}l_{2j+2,\downarrow}^{\dagger}|0\rangle$ form a triplet, i.e. (10) can be obtained by acting with the total spin lowering operator $S^- = \sum_i c_{i,\downarrow}^{\dagger}c_{i,\uparrow}$ on the state $l_{2j,\uparrow}^{\dagger}l_{2j+2,\uparrow}^{\dagger}|0\rangle$. Of course, all states belonging to one triplet have the same energy $2(\mu - 2t_1)$.

We can generalize this procedure to construct the ground states in the subspaces with $n = 3, \dots, N/2$ electrons

$$|\varphi_n^{\uparrow}\rangle \propto l_{2i_n,\uparrow}^{\dagger} \cdots l_{2i_1,\uparrow}^{\dagger}|0\rangle \quad ; \quad H|\varphi_n^{\uparrow}\rangle = n(-2t_1 + \mu)|\varphi_n^{\uparrow}\rangle. \quad (11)$$

They are all degenerate for $\mu = \mu_0 = 2t_1$ and do not feel U . Evidently, they are fully polarized

$$S^z|\varphi_n^{\uparrow}\rangle = \frac{n}{2}|\varphi_n^{\uparrow}\rangle \quad ; \quad \vec{S}^2|\varphi_n^{\uparrow}\rangle = \frac{n}{2} \left(\frac{n}{2} + 1 \right) |\varphi_n^{\uparrow}\rangle. \quad (12)$$

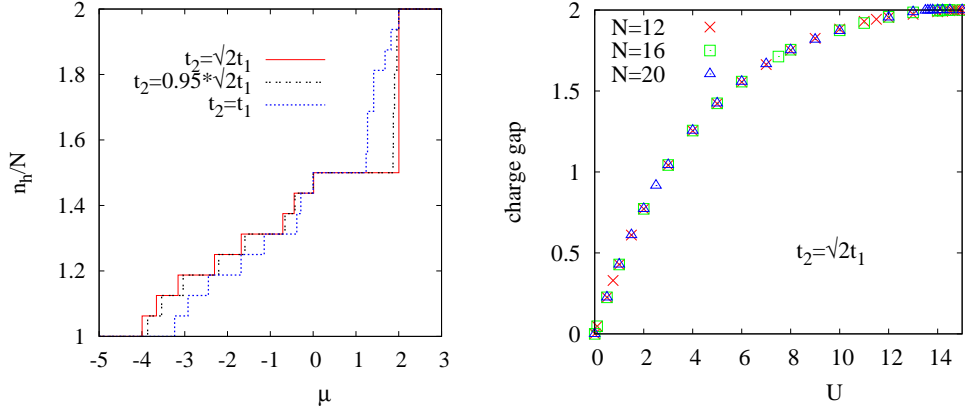


Fig. 5. (Color online) Left: Hole concentration $n_h/N = 2 - n/N$ versus chemical potential μ for $t_2 = \sqrt{2}t_1$ (localized-electron regime), $t_2 = 0.95\sqrt{2}t_1$ and $t_2 = t_1$ for a finite sawtooth chain of $N = 16$ sites (periodic boundary conditions) and $U \rightarrow \infty$, $t_1 = 1$. Right: Charge gap $\Delta\mu = E(N/2 + 1) - 2E(N/2) + E(N/2 - 1)$ at quarter filling versus U for $t_2 = \sqrt{2}t_1$, $t_1 = 1$ and $N = 12, 16, 20$.

Again the application of S^- yields new eigenstates with the same energy and the same \vec{S}^2 , but with $S^z(S^-)^k|\varphi_n^\uparrow\rangle = (n/2 - k)(S^-)^k|\varphi_n^\uparrow\rangle$. Note that $l_{2i_n,\uparrow}^\dagger \cdots l_{2i_k,\downarrow}^\dagger \cdots l_{2i_1,\uparrow}^\dagger |0\rangle$, where $i_1, \dots, i_k, \dots, i_n$ denote n contiguous valleys, is not an eigenstate. Since there is no hard-core rule the maximum filling with localized electrons is $n_{\max} = N/2$, i.e. it is twice as large as for localized magnons.

In the next step we use the fully polarized n -electron states $|\varphi_n^\uparrow\rangle$ to construct the complete set of ground states for $0 \leq n \leq N/2$. The $|\varphi_n^\uparrow\rangle$ can be grouped into two classes, namely in one-cluster states and in multi-cluster states. While for the one-cluster states the electrons occupy a cluster of contiguous valleys, for a multi-cluster state the electrons occupy two or more clusters, where each cluster is built by contiguous valleys and the different clusters are separated by one or more empty valleys. The key observation is that further ground states can be constructed by application of a certain cluster spin flip operator $S_{\text{clust}}^- = \sum_{i \in \text{clust}} c_{i,\downarrow}^\dagger c_{i,\uparrow}$ on a multi-cluster n -electron ground state $|\varphi_n^\uparrow\rangle$. The resulting new states are not fully polarized and complete the set of ground states in each sector n [28].

3.2. Hole concentration in dependence on the chemical potential

In correspondence to the $m(h)$ curve of the Heisenberg model we consider now the hole concentration $n_h/N = 2 - n/N$ in dependence on the chemical potential μ (Fig. 5 (left)). Like for spin systems, see Sec. 2.2, the main characteristics for the system with localized eigenstates (i.e. for $t_2 = \sqrt{2}t_1$) are a size-independent jump of n_h/N from $3/2$ to 2 and a plateau at $n_h/N = 3/2$. This plateau determines the range of validity of the localized-electron picture at $T = 0$. The right panel of Fig. 5 presents the plateau width, i.e. the size of the charge gap, versus U for $N = 12$,

16, and 20. One observes that there is almost no finite-size dependence. Since the charge gap is zero for $U = 0$ and increases with U we conclude that its appearance is due to the on-site repulsion. Small deviations from the ideal parameter values $t_2 = \sqrt{2}t_1$ do not change the n_h/N versus μ curve substantially, as illustrated for the case $t_2 = 0.95\sqrt{2}t_1$ in Fig. 5 (left), whereas for the model with uniform hopping integrals $t_2 = t_1$ the charge gap is significantly smaller and there is no indication of a jump from the plateau at $n_h/N = 3/2$ to $n_h/N = 2$.

3.3. Ground-state residual entropy and low-temperature thermodynamics

The localized-electron states are *linearly independent*, which is connected with the fact (as in the case of spin systems, see Ref. [38]) that the middle site is unique to each valley. Therefore all these highly degenerate states contribute to the partition function. Now the question arises whether the ground state degeneracy can be calculated. Due to the different statistics of Hubbard electrons and Heisenberg spins there are some differences in the construction rules of localized eigenstates (e.g., the occupation of neighboring valleys is forbidden for spins but allowed for electrons, see above). Hence it is not surprising that the ground state degeneracy $g_N(n)$ for n electrons on the N -site sawtooth chain does not coincide with the one for the Heisenberg sawtooth chain (which was equal to the canonical partition functions of n hard dimers on a simple chain of $\mathcal{N} = N/2$ sites, see Sec. 2.3). Nevertheless, $g_N(n)$, $n = 0, 1, 2, \dots, N/2$ for the Hubbard sawtooth chain can also be found by a mapping of the localized-electron degrees of freedom onto the one-dimensional hard-dimer problem. However, this mapping is more intricate and hard dimers have to be considered on a simple chain of N sites (instead of $N/2$ sites as for Heisenberg spins), for details see Ref. [28]. One finds $g_N(n) = Z(n, N)$ for $n = 0, 1, \dots, N/2 - 1$ and $g_N(N/2) = N/2 + 1 = Z(N/2, N) + N/2 - 1$ where $Z(n, N)$ is the canonical partition function of the classical one-dimensional hard-dimer model [46,47]. As for spin systems we can calculate the contribution of localized electron states to the partition function by using this mapping. Again we can present analytical formulas for the low-temperature thermodynamic quantities for a non-trivial quantum many-body problem. The grand-canonical partition function Ξ of the electron system for a chemical potential μ in the vicinity of $\mu_0 = 2t_1$ takes the form

$$\Xi(T, \mu, N) = \lambda_1^N + \lambda_2^N + \lambda_3^N, \\ \lambda_{1,2} = \frac{1}{2} \pm \sqrt{\frac{1}{4} + \exp x}, \quad \lambda_3 = \left(\frac{N}{2} - 1\right)^{\frac{1}{N}} \exp \frac{x}{2}, \quad x = \frac{2t - \mu}{k_B T}. \quad (13)$$

In the thermodynamic limit $N \rightarrow \infty$ only the largest eigenvalue λ_1 of the transfer matrix survives and, using the definitions $S(T, \mu, N) = k_B \partial (T \ln \Xi(T, \mu, N)) / \partial T$, $C(T, \mu, N) = T \partial S(T, \mu, N) / \partial T$, we obtain the following results for the thermody-

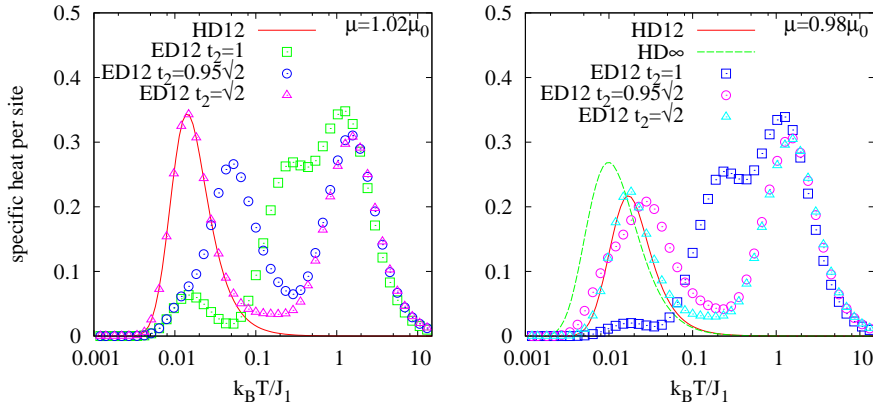


Fig. 6. (Color online) Grand-canonical specific heat per site $C(T, \mu, N)/k_B N$ vs. temperature for the sawtooth Hubbard chain of $N = 12$ sites for two values of μ , $U = \infty$ and $t_1 = 1$, $t_2 = \sqrt{2}$, $0.95\sqrt{2}$ and 1 (symbols). Note that $\mu_0 = 2$ for $t_2 = \sqrt{2}$, $0.95\sqrt{2}$ and 1. For comparison we show the hard-dimer data for $N = 12$ (solid line) which follows from Eq. (13) and for $N = \infty$ (dashed line, Eq. (14)). Note that for $\mu = 1.02\mu_0$ the hard-dimer data for $N = 12$ and $N = \infty$ practically coincide.

namics of one-dimensional hard dimers (see also [28])

$$\begin{aligned} \frac{S(T, \mu, N)}{k_B N} &= \ln \left(\frac{1}{2} + \sqrt{\frac{1}{4} + \exp x} \right) - x \left(\frac{1}{2} - \frac{1}{4\sqrt{\frac{1}{4} + \exp x}} \right), \\ \frac{C(T, \mu, N)}{k_B N} &= \frac{x^2 \exp x}{8 \left(\frac{1}{4} + \exp x \right)^{\frac{3}{2}}}, \\ \frac{\langle n \rangle}{N} &= \frac{1}{2} - \frac{1}{4\sqrt{\frac{1}{4} + \exp x}}, \end{aligned} \quad (14)$$

which are quite similar to the corresponding expressions for Heisenberg spins, see Eq. (7). Again we have a finite residual entropy $S/k_B N = \ln((1 + \sqrt{5})/2) \approx 0.4812$, which is twice as large as for the Heisenberg model.

Results for the low-temperature grand-canonical specific heat are shown in Fig. 6 for two values of the chemical potential slightly above and below μ_0 . Similar as for the spin system we see (i) that the hard-dimer model, Eqs. (13) and (14), yields a good description of the electronic model at low temperatures and (ii) that there is an extra low-temperature maximum in the grand-canonical specific heat due to the manifold of localized electron ground states. Again this additional low-temperature maximum in $C(T)$ disappears at $\mu = \mu_0$ as can be read off from Eq. (14) (note that $C(x = 0) = 0$).

At the end of this section we would like to mention a relation to the so-called

flat-band ferromagnetism in the Hubbard model found by Mielke and Tasaki in the early 1990s [25]. In particular, the ground states belonging to the plateau at $n = N/2$, see Sec. 3.2, are fully polarized ferromagnetic states. For further details of flat-band ferromagnetism in the sawtooth-chain Hubbard model the interested reader is referred to the original papers of Tasaki [25] but also to Ref. [28].

4. Summary

To summarize, we have illustrated some basic concepts of localized eigenstates in correlated systems on highly frustrated lattices and their effect on the low-temperature thermodynamics. As a rule non-interacting electrons or magnons on a lattice are delocalized, i.e. are described by a wave function distributed over the whole lattice. Electrons or magnons may become localized due to randomness or after switching on interactions. As we have discussed on this paper, a frustrating lattice topology may lead to another mechanism for localization. Localized states may survive in the presence of interactions and under certain conditions they can determine the properties of the system at low temperatures.

Acknowledgments

The authors would like to thank J. Jędrzejewski, T. Krokhmalskii, R. Moessner, H.-J. Schmidt, J. Schnack, J. Schulenburg and M. E. Zhitomirsky for useful discussions and fruitful collaboration in this field. A. H. acknowledges financial support by the Deutsche Forschungsgemeinschaft through a Heisenberg fellowship (grant HO 2325/4-1). We mention that most of the numerical results presented in this article were obtained using J. Schulenburg's *spipack*.

1. G. Toulouse, *Commun. Phys.* **2**, 115 (1977).
2. K. Binder and A. P. Young, *Rev. Mod. Phys.* **58**, 801 (1986).
3. P. W. Anderson, *Mater. Res. Bull.* **8**, 153 (1973); P. W. Anderson and P. Fazekas, *Phil. Mag.* **30**, 423 (1974).
4. C. Lhuillier and G. Misguich, in: *High magnetic fields*, C. Berthier, L.P. Lévy, G. Martinez, Eds. (Lecture Notes in Physics, **595**) (Springer, Berlin, 2001), pp. 161-190.
5. J. Richter, J. Schulenburg and A. Honecker, in: *Quantum Magnetism*, U. Schollwöck, J. Richter, D. J. J. Farnell, R. F. Bishop, Eds. (Lecture Notes in Physics, **645**) (Springer, Berlin, 2004), pp. 85-153.
6. P. Lemmens and P. Millet, in: *Quantum Magnetism*, U. Schollwöck, J. Richter, D. J. J. Farnell, R. F. Bishop, Eds. (Lecture Notes in Physics, **645**) (Springer, Berlin, 2004), pp. 433-477.
7. P. Schiffer, *Nature* **413**, 48 (2001).
8. R. Moessner, *Can. J. Phys.* **79**, 1283 (2001).
9. R. Moessner and A. P. Ramirez, *Physics Today*, February 2006, p. 24.
10. *Frustrated Spin Systems*, H. T. Diep, Ed. (World Scientific, Singapore, 2004).
11. *Quantum Magnetism*, U. Schollwöck, J. Richter, D. J. J. Farnell, R. F. Bishop, Eds. (Lecture Notes in Physics, **645**) (Springer, Berlin, 2004).
12. M. Hase, H. Kuroe, K. Ozawa, O. Suzuki, H. Kitazawa, G. Kido and T. Sekine, *Phys. Rev. B* **70**, 104426 (2004); M. Enderle, C. Mukherjee, B. Fåk, R. K. Kremer,

J.-M. Broto, H. Rosner, S.-L. Drechsler, J. Richter, J. Malek, A. Prokofiev, W. Assmus, S. Pujol, J.-L. Raggazzoni, H. Rakoto, M. Rheinstädter and H. M. Rønnow, *Europhys. Lett.* **70**, 237 (2005); M. G. Banks, F. Heidrich-Meisner, A. Honecker, H. Rakoto, J.-M. Broto and R. K. Kremer, *J. Phys.: Condens. Matter* **19**, 145227 (2007); S.-L. Drechsler, O. Volkova, A. N. Vasiliev, N. Tristan, J. Richter, M. Schmitt, H. Rosner, J. Málek, R. Klingeler, A. A. Zvyagin and B. Büchner, *Phys. Rev. Lett.* **98**, 077202 (2007).

13. P. Mendels, F. Bert, M. A. de Vries, A. Olariu, A. Harrison, F. Duc, J. C. Trombe, J. S. Lord, A. Amato and C. Baines, *Phys. Rev. Lett.* **98**, 077204 (2007).
14. K. Takada, H. Sakurai, E. Takayama-Muromachi, F. Izumi, R. A. Dilanian and T. Sasaki, *Nature* **422**, 53 (2003); Y. Wang, N. S. Rogado, R. J. Cava and N. P. Ong, *Nature* **423**, 425 (2003); M. L. Foo, Y. Wang, S. Watauchi, H. W. Zandbergen, T. He, R. J. Cava and N. P. Ong, *Phys. Rev. Lett.* **92**, 247001 (2004).
15. H. N. Kono and Y. Kuramoto, *J. Phys. Soc. Jpn.* **75**, 084706 (2006).
16. H. Tamura, K. Shiraishi, T. Kimura and H. Takayanagi, *Phys. Rev. B* **65**, 085324 (2002); R. Arita, K. Kuroki, H. Aoki, A. Yajima, M. Tsukada, S. Watanabe, M. Ichimura, T. Onogi and T. Hashizume, *Phys. Rev. B* **57**, R6854 (1998).
17. J. Schnack, H.-J. Schmidt, J. Richter and J. Schulenburg, *Eur. Phys. J. B* **24**, 475 (2001).
18. J. Schulenburg, A. Honecker, J. Schnack, J. Richter and H.-J. Schmidt, *Phys. Rev. Lett.* **88**, 167207 (2002).
19. J. Richter, J. Schulenburg, A. Honecker, J. Schnack and H.-J. Schmidt, *J. Phys.: Condens. Matter* **16**, S779 (2004).
20. M. E. Zhitomirsky and A. Honecker, *J. Stat. Mech.: Theor. Exp.*, P07012 (2004).
21. M. E. Zhitomirsky and H. Tsunetsugu, *Phys. Rev. B* **70**, 100403(R) (2004).
22. O. Derzhko and J. Richter, *Phys. Rev. B* **70**, 104415 (2004).
23. M. E. Zhitomirsky and H. Tsunetsugu, *Prog. Theor. Phys. Suppl.* **160**, 361 (2005).
24. O. Derzhko and J. Richter, *Eur. Phys. J. B* **52**, 23 (2006).
25. A. Mielke, *J. Phys. A* **24**, L73 (1991); A. Mielke, *J. Phys. A* **24**, 3311 (1991); A. Mielke, *J. Phys. A* **25**, 4335 (1992); H. Tasaki, *Phys. Rev. Lett.* **69**, 1608 (1992); A. Mielke and H. Tasaki, *Commun. Math. Phys.* **158**, 341 (1993); H. Tasaki, *Prog. Theor. Phys.* **99**, 489 (1998).
26. A. Honecker and J. Richter, *Condensed Matter Physics (Lviv)* **8**, 813 (2005).
27. A. Honecker and J. Richter, *J. Magn. Magn. Mater.* **310**, 1331 (2007).
28. O. Derzhko, A. Honecker and J. Richter, *Phys. Rev. B* **76**, 220402(R) (2007).
29. Z. Gulácsi, A. Kampf and D. Vollhardt, *Phys. Rev. Lett.* **99**, 026404 (2007).
30. C. Wu, D. Bergman, L. Balents, and S. Das Sarma, *Phys. Rev. Lett.* **99**, 070401 (2007); D. L. Bergman and L. Balents, arXiv:0803.3628.
31. H.-J. Schmidt, *J. Phys. A* **35**, 6545 (2002).
32. J. Richter, O. Derzhko and J. Schulenburg, *Phys. Rev. Lett.* **93**, 107206 (2004).
33. J. Richter, J. Schulenburg, A. Honecker and D. Schmalfuß, *Phys. Rev. B* **70**, 174454 (2004).
34. J. Richter, J. Schulenburg, P. Tomczak and D. Schmalfuß, arXiv:cond-mat/0411673.
35. R. Schmidt, J. Richter and J. Schnack, *J. Magn. Magn. Mater.* **295**, 164 (2005).
36. O. Derzhko and J. Richter, *Phys. Rev. B* **72**, 094437 (2005).
37. J. Richter, *Fizika Nizkikh Temperatur (Kharkiv)* **31**, 918 (2005) [*Low Temperature Physics* **31**, 695 (2005)].
38. H.-J. Schmidt, J. Richter and R. Moessner, *J. Phys. A* **39**, 10673 (2006).
39. J. Richter, O. Derzhko and T. Krokhmalskii, *Phys. Rev. B* **74**, 144430 (2006); O. Derzhko, J. Richter and T. Krokhmalskii, *Acta Physica Polonica A* **113**, 433

(2008).

40. J. Schnack, H.-J. Schmidt, A. Honecker, J. Schulenburg and J. Richter, *J. Phys.: Conf. Ser.* **51**, 43 (2006).
41. O. Derzhko, J. Richter, A. Honecker and H.-J. Schmidt, *Fizika Nizkikh Temperatur (Kharkiv)* **33**, 982 (2007) [*Low Temperature Physics* **33**, 745 (2007)].
42. M. E. Zhitomirsky and H. Tsunetsugu, *Phys. Rev. B* **75**, 224416 (2007).
43. A. Honecker, J. Schulenburg and J. Richter, *J. Phys.: Condens. Matter* **16**, S749 (2004).
44. A. Honecker, F. Mila and M. Troyer, *Eur. Phys. J. B* **15**, 227 (2000).
45. F. Mila, *Eur. Phys. J. B* **6**, 201 (1998).
46. M. E. Fisher, *Phys. Rev.* **124**, 1664 (1961).
47. R. J. Baxter, *Exactly Solved Models in Statistical Mechanics* (Academic Press, London, 1982).
48. M. E. Zhitomirsky, *Phys. Rev. B* **67**, 104421 (2003).
49. J. Schnack, R. Schmidt and J. Richter, *Phys. Rev. B* **76**, 054413 (2007).
50. K. Penc, H. Shiba, F. Mila and T. Tsukagoshi, *Phys. Rev. B* **54**, 4056 (1996); H. Sakamoto and K. Kubo, *J. Phys. Soc. Jpn.* **65**, 3732 (1996); Y. Watanabe and S. Miyashita, *J. Phys. Soc. Jpn.* **66**, 2123; Y. Watanabe and S. Miyashita, *J. Phys. Soc. Jpn.* **66**, 3981 (1997).